

P5.7 A COMPREHENSIVE CLIMATOLOGY OF APPALACHIAN COLD AIR DAMMING

Christopher M. Bailey⁺

Gary M. Lackmann⁺

Gail Hartfield*

Kermit Keeter*

*National Weather Service, Raleigh, North Carolina

⁺North Carolina State University

1. Introduction

Cold air damming (CAD) is characterized by the trapping of cold air against the windward side of a mountain range (Richwien, 1980). During CAD, a dome of cold, stable air becomes established along the eastern slopes of the Appalachians and can be identified via characteristic “U-shaped” isobars in the sea-level pressure field. In general, whenever statically stable flow encounters an orographic barrier in a rotating system, upwind ridging and downwind troughing will develop, in part as a manifestation of the geostrophic adjustment process. For the Appalachian Mountains, the result of CAD is a dome of cool, stable air east of the mountains and surface flow that departs from geostrophy. The relative coldness of the CAD “wedge” is the result of (i) along-barrier cold advection, (ii) orographic ascent, and, when sufficient moisture and lift are present, (iii) evaporative cooling and sub-cloud sheltering from insolation. Fritsch et al. (1992) note that clouds and precipitation can play a significant role in the strengthening of CAD through evaporative cooling; near-surface evaporational cooling increases static stability, the degree of orographic blocking, and the strength of CAD.

CAD can have a significant impact on the weather between the crest of the Appalachian Mountains and the coastal plain. The difference in temperature between the damming region (Fig. 1) and the coast can exceed 20°C during strong CAD events (Bell and Bosart, 1988). During the cold season, this can mean the difference between rain and freezing or frozen precipitation.

Operational forecasting experience has demonstrated that CAD events can vary widely in terms of duration, forcing mechanisms, scale, and impact on sensible weather. Accordingly, National Weather Service forecasters in the damming region have identified three categories within an overall CAD spectrum (Hartfield et al., 1996; Kramer, 1997; Hartfield, 1998). The categories originally included:

1.) *Classical damming*: characterized by strong synoptic-scale forcing. A parent high with a central pressure greater than 1028 mb and located north of 40°N latitude is the predominant feature; 2.) *Hybrid damming*: associated with a weaker parent high to the north, and diabatic cooling plays a significant role in complementing the weaker synoptic forcing; 3.) *In-situ damming*: occurs with little or no synoptic-scale support. Diabatic processes are responsible for the development of CAD.

The purpose of this study is to provide an objective climatology of CAD and CAD sub-types. Composites of various meteorological fields are being generated from the climatology, centered at the onset, peak, and demise of various CAD sub-types. It is hoped that these composites will assist forecasters in the recognition of features that are associated with the different CAD sub-types, and with different stages in the evolution of CAD events. For example, a particularly difficult forecasting problem is the demise of CAD; operational numerical models often scour the cold air too quickly. Composites may facilitate identification of the characteristic patterns associated with CAD decay, and allow the signatures common to various sensible weather phenomena to be elucidated.

2. Methodology

An objective CAD detection algorithm was developed in order to capture a broad spectrum of events. Three mountain-normal lines and one mountain-parallel line were chosen, each consisting of three stations (Fig. 1). For the mountain-normal lines, the center station is located within the damming region while the other two are located on either side of the region. Along the three mountain-normal lines, the Laplacian values for sea level pressure and potential temperature are calculated for each hour. The Laplacian values measure the strength of the pressure ridge and the cold dome; negative values in the pressure Laplacian are usually associated with ridging in the center of the section, and a positive potential temperature Laplacian corresponds to colder central values. The fourth line (oriented parallel to the mountains) was chosen to represent the along-barrier pressure gradient.

⁺ *Corresponding author address*: Dr. Gary M. Lackmann, North Carolina State University, Dept. of Marine, Earth and Atmospheric Sciences, Raleigh, NC 27695. email: gary@ncsu.edu

The algorithm requires that the following criteria be met for at least one of the three mountain-normal lines in order for CAD to be identified:

- 1.) The sea level pressure Laplacian must be negative, and exceed in magnitude one standard deviation of all the negative Laplacian values in the dataset.
- 2.) The potential temperature Laplacian must be greater than zero (indicative of cold values in the center).
- 3.) Sea level pressure must be greater at the center station than the other two stations on each line.
- 4.) The difference in pressure along line 4 must be greater than 1.5 mb between either GSP and GSO or GSO and RIC, with higher values to the northeast.
- 5.) All requirements must be present for at least 6 consecutive hours on at least one line.

After the first six hours have passed, requirements 3) and 4) no longer apply in order to allow the demise of an event to be detected.

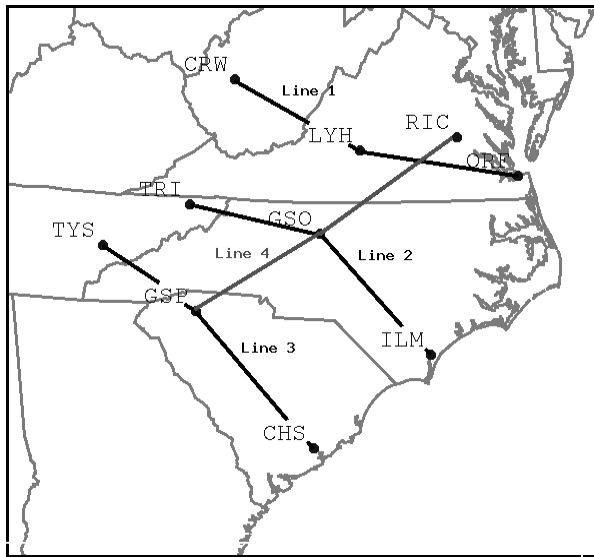


Figure 1. Stations and lines used in the objective CAD detection algorithm.

The detection algorithm was run on hourly surface data over a 12-year period from 1984 to 1995. The hourly surface data were obtained from the National Climatic Data Center's SAMSON (Solar and Meteorological Observation Network) CD-ROM for 1961-1990 and 1990-1995. The hourly data include temperature, dew point, wind speed and direction, hourly precipitation, present weather, and relative humidity. The data were imported into GEMPAK and other parameters such as potential temperature and equivalent potential temperature were calculated. The pressure and temperature time series were smoothed using a 3-point filter to eliminate abnormal data spikes.

After identifying the CAD cases, they were stratified by strength. To rank the cases, six parameters were normalized and then combined into a linear "power ranking" index. The six parameters are:

- 1.) Maximum potential temperature Laplacian;
- 2.) Maximum sea level pressure Laplacian;

- 3.) Average equivalent potential temperature advection along line 4;
- 4.) Maximum number of lines activated by the algorithm
- 5.) Duration of the event;
- 6.) Maximum pressure difference between GSP and RIC.

After the events were ranked, they were divided between cold and warm season, with the "cold season" defined as October 15 to April 15.

In order to stratify the cold season CAD cases, the classifications presented in Hartfield et al. (1996) were applied. It was discovered that further subdivision of the CAD sub-types was required to comprehensively map the spectrum of events. In addition, the "classical" category was sub-divided into dry and precipitating events in order to highlight differences. The CAD cases were therefore divided into the following seven categories:

- 1.) Classical (dry) – At onset, the parent high must be centered north of 40°N latitude with central pressure ≥ 1030 mb. The high must be centered between 100°W and 65°W. The duration of the event must exceed 24 hours with no precipitation falling at the start of the event.
- 2.) Classical (diabatically enhanced) – The same criteria as the dry classical are used except that precipitation is falling at the onset at one of the center stations.
- 3.) Weak Classical – The parent high is either south of 40°N or weaker than 1030mb. There is no precipitation at the start of the event.
- 4.) Hybrid – The same criteria as weak classical except that there is precipitation at the onset at one of the center stations.
- 5.) In-situ – The parent high is centered offshore and south of 40°N, with little or no evidence of a synoptic-scale contribution to CAD. Precipitation is observed at the start of the event at one of the center stations.
- 6.) Cyclonic – A cyclone to the south, rather than an anticyclone to the north, is the predominant feature in the damming region. The cyclone is characterized by a greater number of closed isobars at the initial time than the parent high to the north.
- 7.) Unknown – All cases that do not fit into one of the above categories.

Composites based on the above classifications were generated to describe the synoptic-scale flow pattern. The data used for compositing are the NCEP Reanalysis grids, provided by the NOAA-CIRES Climate Diagnostics Center, Boulder, CO, USA (<http://www.cdc.noaa.gov>). The NCEP reanalysis data possess 6-hour temporal resolution, 2.5° by 2.5° horizontal resolution, 17 isobaric levels, plus near-surface and sea-level fields. The grids were transferred into GEMPAK format for use in this study. Additional details regarding a similar compositing system may be found in Lackmann et al. (1996). Three different "center times" (corresponding to three separate composites) were used for each CAD sub-type. These include (i) a composite centered at CAD onset (defined as the hour of first detection), (ii) a composite centered at the peak of CAD strength (defined by the peak pressure Laplacian), and (iii) a composite centered at the demise of

CAD (defined as the last hour of detection). In order to establish consistency between the hourly data employed by the CAD detection algorithm and the 6-hourly NCEP grids, the closest 00, 06, 12, or 18 UTC time to the center time of a given event is denoted $T = 0$. The composites each span the period from $T-96$ to $T+96$ hours about the central time. It is important to note that individual CAD cases will exhibit variability about the composite due to “smearing”, which increases away from the center time. The composites are designed to identify synoptic-scale common denominators between the various events.

The composited fields include sea level pressure, 500-mb geopotential height, 500-mb geopotential height anomalies, and the anomaly significance field. Anomalies are defined as the departure of the composites means from the weighted monthly climatological fields. The climatological fields are constructed from monthly means weighted by the number of cases in a particular month. A two-sided *student-t* test is performed on the composites to determine their statistical significance. The significance of a composited feature will generally decrease as the offset from the central time increases.

3. Results

The detection algorithm was run over a 12-year period spanning the years from 1984 to 1995. In that period, a total of 374 CAD cases were identified. Of those cases, 194 occurred in the cold season and 180 occurred in the warm season. The monthly distribution of CAD cases is presented in Fig. 2. The frequency of damming events peaked in September, averaging 3.5 events per month. The lowest CAD frequency was found during July, which averaged less than 1 event per month. March exhibited the highest CAD frequency during the cold season, averaging over 3 events per month. The minimum in July is consistent with the 50-yr climatology presented by Bell and Bosart (1988), however they found March to be the month with the highest damming frequency. The similarity in the

number of warm- and cold-season events is perhaps surprising, and will be discussed further below.

Using the aforementioned “power rankings” to determine the relative strength of the events, we find that the strongest events occur more often in the cold season. 51% of all cold season events were ranked in the top 150 events. On the other hand, 54% of all warm season events were ranked in the bottom 150 events. Another means of quantifying the relative weakness of the warm-season events is to display the average number of “top-200” CAD events per month, which is also presented in Fig. 2. It is evident that the frequency of strong events was greatest during the winter months of February and March. June, July and August were characterized by a larger number of weaker events.

An example composite centered at the peak CAD strength for the “dry classical” category is presented in Fig. 3, which depicts the composite of sea-level pressure and 500-mb geopotential height. This composite consists of a total of 23 cold-season cases. The composite “parent high” is centered over southern Quebec, with a central pressure in excess of 1032 mb. Ridging east of the Appalachian Mountains is evident in Virginia, the Carolinas, and Georgia. Off the coast, a trough signature is present in the sea level pressure field. This is a reflection of the coastal front, which forms the eastern periphery of the cold dome in many CAD events. At the 500-mb level, confluence is present above the surface high-pressure system, and a short-wave ridge is centered to the west of the surface high. Figure 4 depicts the 500-mb geopotential height composite anomaly and its statistical significance. The positive anomaly in the ridge over the eastern half of the United States exceeds 10 dam in magnitude and exhibits 99% significance. Two significant troughs are present at the 500-hPa level, including one to the northeast of the damming region over the Canadian Maritimes, and another over the southwestern United States.

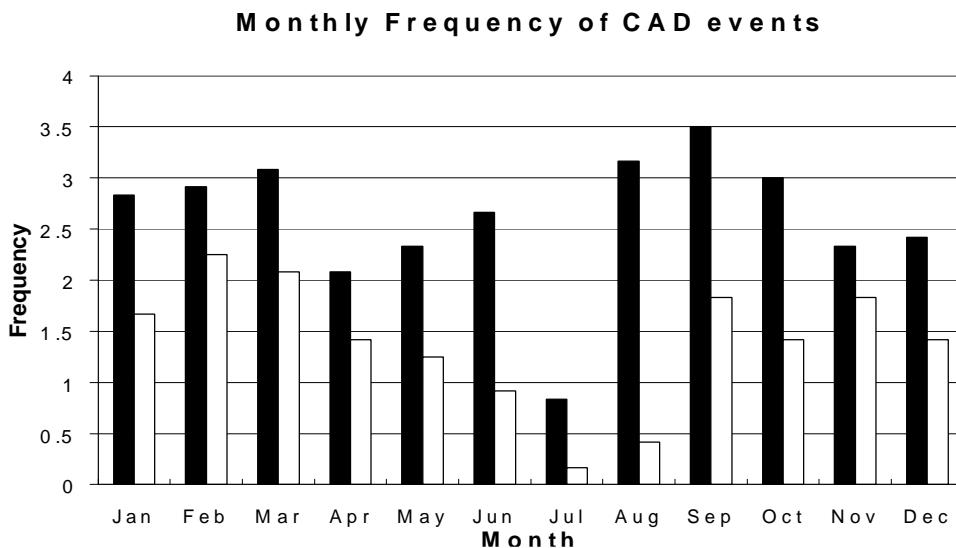


Figure 2. The average number of CAD events per month determined from the detection algorithm (black) and average number on top 200 CAD events determined from “power rankings” (white) between 1984 and 1995.

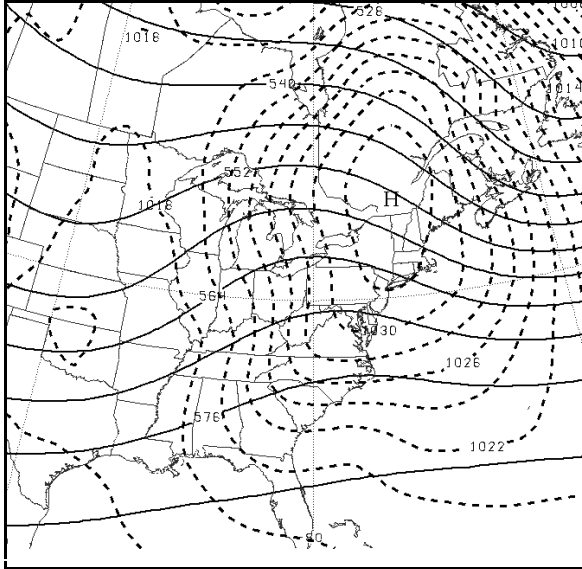


Figure 3. Classical (dry) composite of sea level pressure (dashed lines, contour interval 2 mb) and 500-mb geopotential height (solid lines, contour interval 6 dam). The composite is centered on CAD peak and is for $T = 0$.

Figures 5 and 6 display results of a 45-case composite of diabatically enhanced classical CAD events. Comparison of the dry classical with the diabatically enhanced classical composite reveals subtle differences in the sea-level pressure field (cf. Figs. 3 and 5). In the dry composite, ridging extends farther south into Georgia and Alabama, and is also more pronounced over the offshore waters east of the damming region. At the 500-mb level, stronger ridging is evident for the dry composite; the relatively straight confluent flow evident in the diabatically

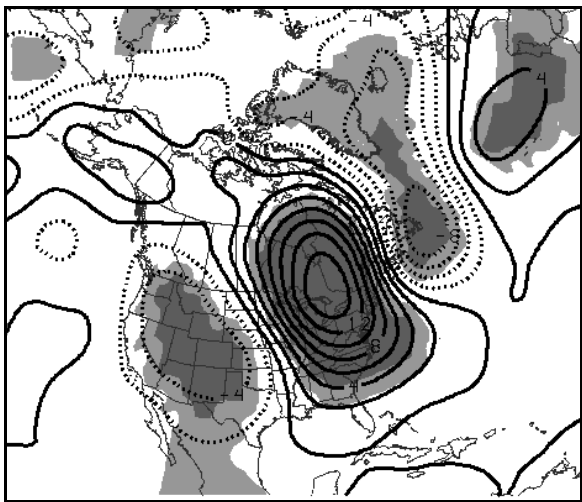


Figure 4. Classical (dry) composite 500-mb geopotential height anomaly (interval 2 dam) and statistical significance as determined from a 2-sided *student-t* test (shaded areas). Solid lines represent positive anomalies and dashed lines correspond to negative anomalies. Lightly shaded areas indicate 95% significance and the darkly shaded areas indicate 99% significance. The time of the composite corresponds to that shown in Fig. 3.

enhanced composite may correspond to a more pronounced jet entrance signature (Figs. 3 and 5). There is also stronger evidence for a southern stream left jet exit in the diabatically enhanced composite relative to the dry composite (Fig. 5). The 500-hPa anomaly fields also exhibit differences (cf. Figs. 4 and 6). In the diabatically enhanced case, the troughing over the southwestern U.S. is weaker and not statistically significant, and the positive anomaly corresponding to the ridge is weaker and more zonally elongated (Fig. 6). This is consistent with less ridging, and possibly with more progressive disturbances in an active southern branch of the jet stream.

4. Ongoing Research

Currently, the CAD classification scheme is being finalized. Composites will continue to be generated for all CAD sub-types, and for a variety of atmospheric fields. Other stratification schemes are under consideration, including a stratification by sensible weather at stations such as Raleigh and Greensboro, NC. We are open to additional suggestions for operationally relevant stratification schemes. The results of these composites will be available via the internet in the near future.

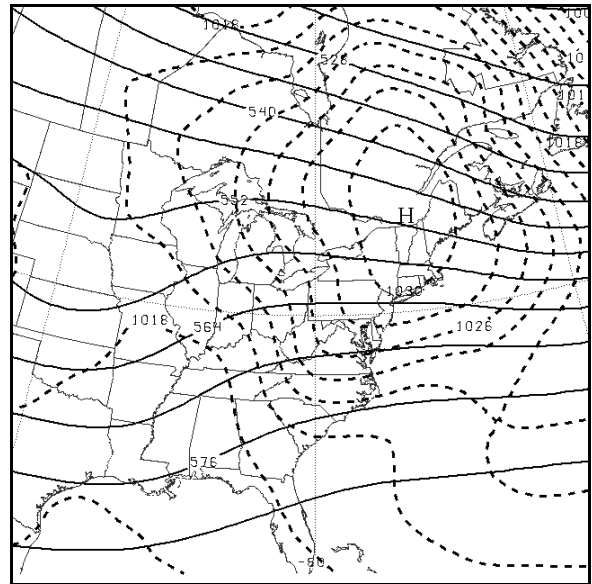


Figure 5. As in Fig. 3, except for diabatically enhanced classical.

5. Acknowledgements

This research was supported by the NOAA Collaborative Scientific, Technology, and Applied Research (CSTAR) Program grant, NA-07WA0206. We wish to acknowledge Larry Lee, Scott Sharp, Jonathan Blaes, Neil Stuart, Hugh Cobb, Reid Hawkins, Carin Goodall, and other personnel with the five NWS offices involved in this project (Raleigh, Wilmington, and Newport, NC; Greer SC; Wakefield, VA) for helpful insights and discussions concerning the CAD problem. We also wish to thank Al Riordan of NCSU for

useful suggestions during the development of the CAD detection algorithm.

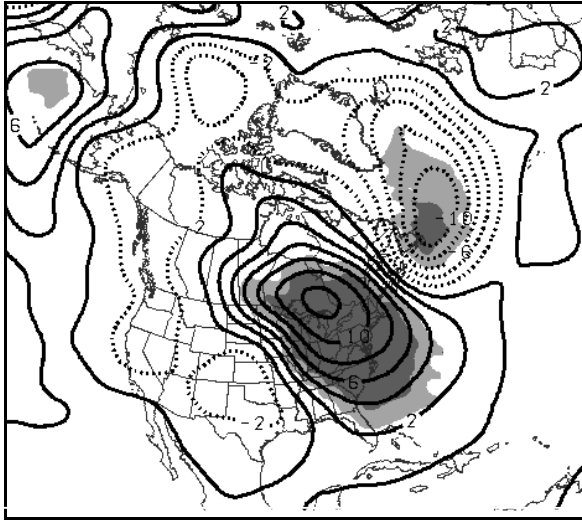


Figure 6. As in Fig. 4, except for diabatically enhanced classical.

6. References

- Bell, B. D. and L. F. Bosart, 1988: Appalachian cold-air damming. *Mon. Wea. Rev.*, **116**, 137–161.
- Fritsch, J. M., J. Kopolka, and P. A. Hirschberg, 1992: the effects of subcloud-layer diabatic processes on cold air damming. *J. Atmos. Sci.*, **49**, 49–70.
- Hartfield, G., K. K. Keeter, and P. Badgett, 1996: Spectrum of cold-air damming and damming lookalikes, *unpublished*, [Available from the Raleigh National Weather Service Office, Raleigh, NC].
- Hartfield, G., 1998: Cold air damming: An introduction. *National Weather Service Eastern Region Training and Evaluation Module No. 4*. [Available online from <http://www.nws.noaa.gov/er>].
- Kramer, D. 1997: Real-time mesoscale model evaluation during Appalachian cold air damming. M. S. Thesis, Dept. of Marine, Earth, and Atmospheric Sciences, North Carolina State University, 139 pp.
- Lackmann, G. M., L. F. Bosart, and D. Keyser, 1996: Planetary- and synoptic-scale characteristics of explosive wintertime cyclogenesis over the western North Atlantic Ocean. *Mon. Wea. Rev.*, **124**, 2672–2702.
- Richwien, B. A., 1980: The damming effect of the southern Appalachians. *Natl. Wea. Dig.*, **5**(1), 2–12.